TISSUE ENGINEERING: Part A
Volume 22, Numbers 21 and 22, 2016

DOI: 10.1089/ten.tea.2016.0032

termis
Tissue Engineering
& Regenerative Medicine
International Society

ORIGINAL ARTICLE

Stabilized Collagen and Elastin-Based Scaffolds for Mitral Valve Tissue Engineering

Christopher Deborde, BS,[1] Dan Teodor Simionescu, PhD,[1] Cristopher Wright, MD,[2] Jun Liao, PhD,[3] Leslie Neil Sierad, PhD,[1] and Agneta Simionescu, PhD[1]

There is a significant clinical need for new approaches to treatment of mitral valve disease. The aim of this study was to develop a tissue-engineered mitral valve scaffold possessing appropriate composition and structure to ensure ideal characteristics of mitral valves, such as large orifice, rapid opening and closure, maintenance of mitral annulus–papillary muscle continuity, *in vivo* biocompatibility and extended durability. An extracellular matrix-based scaffold was generated, based on the native porcine mitral valve as starting material and a technique for porcine cell removal without causing damage to the matrix components. To stabilize these structures and slow down their degradation, acellular scaffolds were treated with penta-galloyl glucose (PGG), a well-characterized polyphenol with high affinity for collagen and elastin. Biaxial mechanical testing presented similar characteristics for the PGG-treated scaffolds compared to fresh tissues. The extracellular matrix components, crucial for maintaining the valve shape and function, were well preserved in leaflets, and in chordae, as shown by their resistance to collagenase and elastin. When extracted with strong detergents, the PGG-treated scaffolds released a reduced amount of soluble matrix peptides, compared to untreated scaffolds; this correlated with diminished activation of fibroblasts seeded on scaffolds treated with PGG. Cell-seeded scaffolds conditioned for 5 weeks in a valve bioreactor showed good cell viability. Finally, rat subdermal implantation studies showed that PGG-treated mitral valve scaffolds were biocompatible, nonimmunogenic, noninflammatory, and noncalcifying. In conclusion, a biocompatible mitral valve scaffold was developed, which preserved the biochemical composition and structural integrity of the valve, essential for its highly dynamic mechanical demands, and its biologic durability.

Keywords: mitral valve prolapse; matrikines; bioreactor

Introduction

The mitral valve (MV) is a complex structure that opens during diastole and closes in systole, allowing the passage of blood from the left atrium to the left ventricle, and blocking the blood backflow under the high-pressure environment in the left ventricle. The components of MV apparatus that coordinate their movement to ensure the normal functioning of the valve are two leaflets with different shapes, the saddle-shaped annulus, the chordae tendinae, and the papillary muscles. The anterior leaflet is positioned in a fibrous continuity (fibrous annulus) with the noncoronary leaflets of the aortic valve, while the posterior leaflet is attached through the muscular part of the annulus to the left ventricle. The leading edges of both leaflets are reinforced by flexible chordae tendinae, which continue with the papillary muscles.[1] The annulus-papillary muscle continuity is essential for valve mechanics.

The biochemical composition is fundamental for the MV mechanical demands, and its durability.[2] There are three layers in the structure of MV leaflets: the *fibrosa*, a stiff layer on the ventricular surface, composed of a thick, organized collagen fibers; *atrialis*, a more compliant thin layer on the atrial surface, composed mainly of elastic fibers; and *spongiosa*, rich in glycosaminoglycans (GAG) and proteoglycans.[3] There is also a thin layer of linearly arranged elastic fibers on the ventricular side, continuous with the elastic layer of the chordae tendinae. The chordae are composed of highly crimped collagen fibers, and elastin. The valve homeostasis is maintained by valvular interstitial

[1]Department of Bioengineering, Clemson University, Clemson, South Carolina.
[2]Department of Cardiothoracic Surgery, Greenville Memorial Hospital, Greenville, South Carolina.
[3]Department of Agricultural and Biological Engineeering, Mississippi state university, Starkville, Mississippi.

cells (VICs), able to adapt to pressure and to respond to environmental changes, remodeling the valve and maintaining its strengths and durability.[3–5] The mechanical stress is transmitted to VICs through their interactions with the extracellular matrix (ECM) (mechanotransduction).[6–10] The MV surface is covered with endothelial cells, which interact with VICs to maintain the integrity of valves and also regulate the leaflets' mechanical properties.[11]

MV insufficiency leading to regurgitation affects >2% of the population and, most frequently, is caused by mitral valve prolapse (MVP).[12,13] MVP is mainly due to myxomatous degeneration, leading to altered mechanical stress and turbulent flow in the proximity to the MV leaflets.[3,14,15] MVP is characterized by enlarged and thickened ''floppy'' leaflets, associated with chordal elongation, thinning, and/or rupture,[16] and severe annular dilatation, with varying degrees of calcification.[17] Myxomatous changes consisting of proteoglycan and GAG accumulation are observed mainly in the *spongiosa*, and extend diffusely to the other layers, resulting in severe disruption of collagen organization in the *fibrosa*, the structural core of the MV leaflets, contributing to weakening of the floppy MV. The elastic fibers are fragmented in the *atrialis*, with occasional calcification.[18] GAG accumulation in myxomatous chordae is associated with elastic fiber deficiency.[19,20] VICs, as a result of exposure to TGF-β1 and oxidative stress are activated to myofibroblasts, with increased expression of matrix metalloproteinases (MMPs) and cathepsin K that contribute to degeneration.[21–25] Active MMPs degrade ECM components, releasing bioactive fragments (matrikines) and TGF-β1, leading to further VIC activation, fibrosis, and calcification.[6,26,27]

MV disease is presently treated successfully by surgical replacement or repair. However, prosthetic valve replacements have a limited lifespan and surgical repairs are technically demanding and inherently associated with high rate of MVP reoccurrence. Therefore, there is a significant clinical need for new approaches to treatment of MV disease. One such solution might be provided by tissue engineering and regenerative medicine approaches utilizing scaffolds, cells, and bioreactors.[28] Our goal is to develop a tissue-engineered MV possessing appropriate composition, structure, and function with the ''ideal'' characteristics of MV: large orifice, rapid opening and closure, no rigid support, maintenance of mitral annulus–papillary muscle continuity, extended durability, biocompatibility, normal function at any change in the left ventricle (LV) size in time, and also, easy to produce and construct.[29] As the integrity of ECM components is critical for the complex functioning of the MV, we aim to develop a collagen and elastin-based scaffold based on the native porcine MV, as starting material, and a technique to remove the porcine cells without damaging the matrix components.

Notably, since ECM proteins are largely conserved among species, properly decellularized xenogeneic tissues are not considered immunogenic and could serve as excellent scaffolds for regenerative medicine efforts. FDA has already approved several acellular ECM-derived tissues from bovine and porcine sources for human surgical use such as injectable collagen, acellular dermis, intestinal submucosa, pericardium, and fascia lata. To date it is estimated that at least 5 million patients have received such implants without signs of rejection.

To stabilize the matrix components and slow down their degradation, we will treat the scaffolds with penta-galloyl glucose (PGG), a well-characterized polyphenol with high affinity for collagen and elastin.[30–32] PGG has been reported to have many beneficial effects, such as antioxidant, anti-inflammatory, and anticalcification properties.[33–35] We hypothesize that PGG, by virtue of its collagen and elastin-stabilizing abilities will preserve the composition and structure of the valve ECM, and protect the scaffold from matrix peptide liberation and cell activation.

Materials and Methods

MV decellularization

Porcine MVs were collected from a local abattoir and transported to the laboratory on ice. After cleaning and trimming extraneous heart muscle, the valves were immersed in ddH_2O overnight at 4°C to induce hypotonic shock and cell lysis. The next day, the valves were treated with NaOH 0.05 M for 2 h, then incubated for 5 days under agitation, in a solution containing 0.2% SDS, 1% Triton X-100, 1% deoxycholic acid, and 0.4% EDTA, prepared in 20 mM Tris pH 7.4. To remove the detergents, the valves were rinsed 10 times for 15 min with ddH_2O, then treated with 70% ethanol for 20 min to reduce the bio-burden, and rinsed again 4 times for 15 min with ddH_2O. Nucleic acid removal was completed by incubation in a 720 mU/mL deoxyribonuclease, 720 mU/mL ribonuclease mixture in PBS for 2 days at 37°C. Finally, scaffolds were rinsed in ddH_2O (three times for 15 min), and incubated in 70% ethanol overnight at room temperature. The MV scaffolds were stored in sterile PBS with 1% protease inhibitors and 1% antibiotic/antimycotic (Pen-Strep) at 4°C.

DNA extraction

DNA was isolated from tissues ($n = 10$) following the instructions provided in the DNeasy® Blood & Tissue Kit from Qiagen. DNA was then analyzed by ethidium bromide agarose gel electrophoresis, using the Sub-Cell® GT electrophoresis instruments and instructions (170-4402) provided by BioRad. DNA bands were measured by densitometry in a BioRad Gel Imager.

Histology and immunohistochemistry

Rehydrated paraffin sections (5 μm) were stained with hematoxylin and eosin (H&E), Movat's pentachrome, and Verhoeff-Van Gieson, according to the instructions in the kits purchased from Poly Scientific R&D Corp. 4′,6-Diamidino-2-phenylindole (DAPI) was purchased from Sigma-Alridch Corporation. Immunohistochemistry (IHC) was performed on formalin-fixed and paraffin-embedded sections using heat-mediated antigen retrieval (10 mM citric acid at pH of 6, for 10 min at 90°C), followed by exposure to 0.025% Triton X-100 for 5 min. After incubation in normal blocking serum for 45 min, the primary antibodies diluted to 2 μg/mL were applied overnight at 4°C in a humidified chamber. The following antibodies were used: rabbit anti-Collagen IV (Ab6586; Abcam), rabbit anti-Laminin (Ab11575; Abcam), rabbit anti-Vimentin (Ab92547; Abcam), rabbit anti-α-Smooth Muscle Actin (Ab5694; Abcam), and rabbit anti-Integrin β1 (Ab52971; Abcam). Negative controls were

obtained by omitting the primary antibodies. The Vectastain Elite kit and the ABC diaminobenzidine tetrahydrochloride peroxidase substrate kit were purchased from Vector Laboratories. Sections were counterstained with a diluted hematoxylin before mounting. Images were obtained at various magnifications on a Zeiss Axiovert 40CFL microscope using AxioVision Release 4.6.3 digital imaging software (Carl Zeiss MicroImaging, Inc.).

PGG treatment

High-purity 1,2,3,4,6-Penta-O-galloyl-beta-D-glucose (PGG) was a generous gift from N.V. Ajinomoto OmniChem S.A., Wetteren, Belgium (www.omnichem.be). The acellular scaffolds were treated with sterile 0.3% PGG in 50 mM Na_2HPO_4, 0.9% NaCl, pH 5.5 containing 20% isopropanol overnight at room temperature under agitation and protected from light. Scaffolds were then rinsed with sterile PBS three times, and then stored in sterile PBS with 1% protease inhibitors and 1% antibiotic/antimitotic (Pen-Strep).

Resistance to collagenase and elastase

Tissue degradation by collagenase and elastase was described previously.[36] Briefly, ~15 mg scaffold fragments were lyophilized and the dried samples weighed. The samples were then incubated with 1 mL of 6.25 U/mL type 1 collagenase in 100 mM Tris, 1 mM $CaCl_2$, and 0.02% NaN_3, pH 7.8 at 37°C, for 24 and 48 h with agitation ($n=6$ per group). Similarly, 10 U/mL elastase was used to test elastin stabilization. After removing the enzymes by centrifugation and rinsing in ddH_2O, the samples were lyophilized and weighed. Resistance to enzymes was calculated as percent weight loss.

Detection of soluble matrix peptides

Scaffold samples were pulverized in liquid nitrogen and extracted in 50 mM Tris-HCl, 150 mM sodium chloride (NaCl), 1 mM EDTA, 1% Triton X-100, 1% sodium deoxycholate, 0.1% sodium dodecyl sulfate, pH 7.4, and 10 μL/mL protease inhibitor cocktail, for 16 h, followed by 15 min centrifugation at 12,000 rpm at 4°C. Protein content was determined using the bicinchoninic assay (BCA) and 15 μg from each sample were loaded on 4–15% SDS polyacrylamide gels. After electrophoresis, the gels were stained using the silver staining method.[33] BCA protein assay kit and the silver stain kit (Silver Snap) were purchased from Pierce Biotech (Thermo Scientific).

Mechanical testing

The evaluation of biaxial mechanical properties of valve tissues was described previously.[37] Briefly, square tissue samples (~12×12 mm) were trimmed from the anterior leaflet with one edge of the sample aligned along leaflet circumferential direction and the other edge aligned along leaflet radial direction. Thickness of each sample was measured three times using a digital caliper. Four markers were placed in the center of the sample and were tracked with a CCD camera to obtain biaxial tissue deformation. Samples were attached to eight loops of 000 polyester suture of equal length via stainless steel hooks (two loops each edge) and mounted on the biaxial testing system. Membrane tension (force/unit length) was applied along each orthogonal axis (aligned with circumferential direction or radial direction of tissue sample), and was ramped slowly from a 0.5 N/m preload to a peak tension of 60 N/m. For testing, tissue sample was preconditioned for 10 continuous cycles and followed by a 60 N/m equibiaxial tension protocol. Maximum stretch ratios along the circumferential direction (λ_{circ}) and radial direction (λ_{rad}) were used to assess the tissue extensibility. The biaxial testing was performed with samples immersed in a PBS bath (pH 7.4). For tensile testing, 50 mm long samples were cut and thickness was measured using digital calipers. Samples were analyzed at a constant uniaxial velocity of 0.1 mm/s until failure using a 10 Newton load cell on a Synergie 100 testing apparatus (MTS System Corporation).

Differential scanning calorimetry

Thermal denaturation temperature (T_d), was determined by differential scanning calorimetry (DSC, model 131; Setaram Instrumentation) at a heating rate of 10°C/min from 20°C to 110°C in a N_2 gas environment. T_d was defined as the temperature at the endothermic peak.[38]

Cell seeding and cytocompatibility

PGG-treated scaffolds were equilibrated overnight in DMEM with 50% FBS, 1% antibiotics and seeded with human adipose tissue-derived stem cells (ASCs) internally and externally. For internal seeding, the base and free edges of the leaflets were inflated with sterile compressed air using a 33GA×1½-inch needle, and then injected with 0.5 mL of a 1×10^6 cells/mL cell suspension. For external seeding, a 0.5 mL of 1×10^6 cells/mL cell suspension was added dropwise to scaffolds and cells allowed to adhere for 1 h; then each scaffold was submerged in media (DMEM with 50% FBS, 1% antibiotics, sterile filtered) and statically incubated for 3 days. The viability of the cells after incubation was tested using the Live/Dead Viability/Cytotoxicity Assay Kit (Invitrogen) was used.

In a separate experiment, circular punches of PGG-treated and untreated scaffolds ($n=4$) were seeded with human cardiac fibroblasts (200,000 per sample) and incubated in DMEM, 10% FBS, 1% antibiotics for 1 week. Scaffolds were then evaluated for the expression of α-smooth muscle cell actin (α-SMA) by IHC, TGF-β by ELISA, and MMPs by gelatin zymography.

Bioreactor conditioning

PGG-treated scaffolds ($n=3$) were seeded with 4×10^6 cells per leaflet and mounted in bioreactors, originally developed in house[39] and now commercially available from Aptus, LLC. The number of cells seeded was determined based on a study using concentrations of cells ranging from 5×10^6 cells to 1×10^6 cells injected per leaflet (not shown). The bioreactors were filled with DMEM, 10% FBS, 1% antibiotics and placed within a standard cell culture incubator maintained at 37°C, 90% humidity, and 5% CO_2. Cell culture media was replaced every 3–4 days. Pressures were slowly increased from 1/5 mmHg (diastolic/systolic) to about 10/170 mmHg (diastolic/systolic) over 1 week to allow cells to adapt to the new dynamic environment.

TGF-β1 assay

Tissue samples (0.5 cm circular punches) were pulverized in liquid nitrogen and extracted in RIPA buffer (0.1% SDS, 1% sodium deoxycholate, 1% Triton X-100, 1 mM EDTA in 150 mM Tris-HCl, 150 mM NaCl, pH 7.4, and 1% protease inhibitor cocktail) for 16 h at 4°C. Total protein content was evaluated by BCA and extracts were analyzed for TGF-β1 content using an ELISA kit from Abcam (Ab100647).

Gelatin zymography

MMP activity was determined by gelatin zymography: 6 μg proteins/lane were loaded in triplicates on ready to use BioRad gels, alongside prestained molecular weight standards. After development and staining with Coommassie Blue, the MMP clear bands on a dark blue background were evaluated by densitometry and expressed as relative density units. Electrophoresis apparatus and imager, chemicals, and molecular weight standards were all purchased from Bio-Rad.

In vivo *biocompatibility*

Acellular leaflet and chordae scaffold samples, treated with PGG and nonPGG-treated were prepared as described above. A 10 mm diameter sterile biopsy punch was then used to cut equally sized leaflet samples for implantation. Before implantation, the samples were sterilized in 0.1% (w/v) peracetic acid in PBS for 1 h, followed by rinsing in four changes of sterile PBS.

In accordance with an IACUC-approved animal use protocol, 24 juvenile Sprague-Dawley rats (cca. 50 g weight) were used for this study. Rats were shaved and prepped for surgery, anesthetized, and a 1 cm incision was made in the dorsal area of each rat. Using blunt dissection, two subdermal pockets were created and one sample was then inserted into each pocket (total $n = 2$ implants per rat) and the incisions were closed using surgical staples. Thus, each group of implants ($n = 12$ samples for leaflet, chordae, with and without PGG treatment) were implanted into randomly selected $n = 6$ rats. Rats were allowed to recover and maintained in standard housing conditions with food and water *ad libitum*. Rats were euthanized at 4 weeks via CO_2 gas in an Euthanex system followed by bilateral pneumothorax. Scaffold samples were explanted, fixed in 10% neutral buffered formalin, and processed for histological examination of cell infiltration using Masson's trichrome stain and for T-lymphocytes using IHC for CD8 as described above. Micrographs (10 images/group) were digitized and cell nuclei within Trichrome-stained sections and CD8-positive cells were counted using Image J software.

Statistical analysis

Results are expressed as mean ± standard deviation. Statistical analysis was performed using one-way analysis of variance (ANOVA). Differences between means were determined using the least significant difference with an alpha value of 0.05.

Results

Scaffold preparation

Porcine MVs were treated with alkali, detergents, and nucleases to remove the cells, but to maintain the fibrous matrix composition of leaflets and chordae; the resulting scaffold preserved all the valve components (Fig. 1A). To visualize the elimination of cells, sections of scaffolds and fresh MVs (leaflets and chordae) were stained with H&E and DAPI, which confirmed the complete removal of cellular components (Fig. 1C). To further validate the completeness of decellularization, DNA was extracted from scaffolds and compared to the DNA content of fresh MV tissues (Fig. 1B). Ethidium bromide-agarose gel electrophoresis followed by quantitative densitometry showed 98% elimination of DNA from leaflets and 99% from chordae.

Evaluation of scaffold structure and matrix integrity

Collagen and elastin fibers, both crucial for maintaining valve shape and function, maintained their integrity in both leaflets and chordae after decellularization, as observed in sections stained with Movat's Pentachrome (Fig. 2A, F). Voerhoff van Gieson (VVG), a specific stain for elastin, showed intact elastin fibers in the atrial and ventricular side, and in the structure of chordae (Fig. 2B, E). GAG were removed together with the cells, forming typical ''pores'' in the tissue, necessary for cell repopulation. Basal lamina components, collagen IV and laminin, essential for cell adhesion, were detected using specific antibodies (Fig. 2C, D).

Scaffold stabilization and cross-linking evaluation

The acellular scaffolds were treated with 0.05% PGG to stabilize the tissues and increase their strengths and resistance to degradation. Biaxial testing showed that decellularization significantly decreased the tissue stiffness in both the radial and circumferential directions, compared to fresh tissues (Fig. 3A, B). Treatment with PGG, a polyphenolic compound that binds to proline-rich regions and induces the formation of cross-links within the collagen and elastin molecules, contributed to the increase of tissue stiffness, showing a doubling in elastic modulus (from 23.4 ± 4 to 49.7 ± 7 MPa). DSC showed a slightly lower but statistically significant denaturation temperature (T_d) for decellularized scaffolds when compared to the fresh tissue (66.4°C ± 6°C vs. 70.7°C ± 8°C) due to tissue destabilization after removal of cells. PGG-treated scaffolds exhibited significantly higher T_d (84.5°C ± 9°C) possibly due to the increase in number of cross-links (Fig. 3D).

The efficiency of acellular MV and chordae scaffold stabilization with PGG was evaluated by analyzing their resistance to collagenase and elastase. Untreated scaffolds and fresh MV tissues were used as controls. Results showed that acellular scaffolds were more readily degradable by both enzymes as compared to fresh tissues (Fig. 4). Also, treatment with PGG significantly reduced their susceptibility to enzymes: by fivefold to collagenase (Fig. 4A) and more than twofold to elastase (Fig. 4B).

To evaluate the degradability of matrix components, PGG-treated scaffolds and controls were extracted in a detergent-rich RIPA buffer and the soluble peptides released were detected by SDS-PAGE electrophoresis (Fig. 7D). Compared to nontreated scaffolds, the PGG-treated scaffolds released significantly lower amounts of soluble protein fragments.

Cell seeding and cytocompatibility

The acellular MV scaffolds exhibited excellent compatibility toward ASCs as demonstrated by the presence of viable

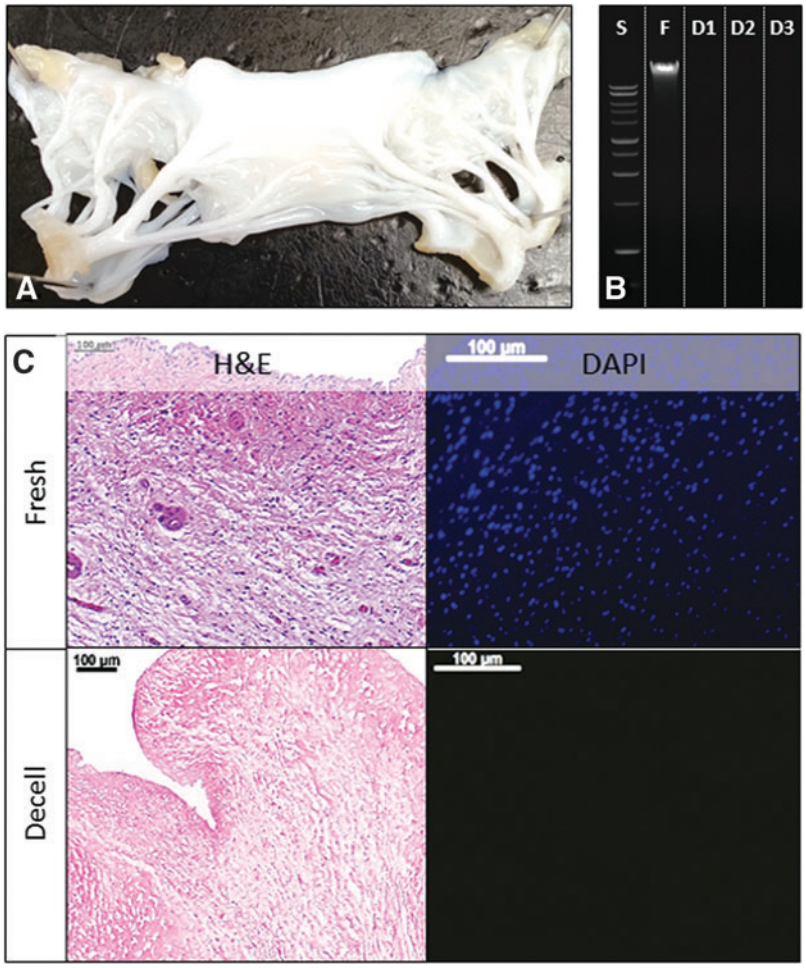

FIG. 1. Mitral valve decellularization. **(A)** Macroscopic aspect of a decellularized mitral valve leaflet. **(B)** Ethidium bromide agarose gel electrophoresis analysis of DNA extracted from fresh tissue (F) and decellularized valve tissue (D1-3); S, DNA ladder standard. **(C)** Representative histology analysis of fresh and decellularized (Decell) mitral valve stained with H&E and DAPI. Bars in (**C**) are 100 µm. H&E, hematoxylin and eosin. Color images available online at www.liebertpub.com/tea

cells after 3 days of incubation under static conditions (Fig. 5B). Cells spread between the fibers of leaflets, as seen in the DAPI, H&E, and Movat's Pentachrome-stained sections. Images show the presence of vimentin, a protein known to be secreted by mesenchymal cells (Fig. 5D). Cells seeded on the surface maintained their viability and attachment to the valve.

Bioreactor studies

Cell-seeded, PGG-treated MV scaffolds were dynamically conditioned in heart valve bioreactors. After 3 weeks of bioreactor testing, the cells were viable (Fig. 6C) and showed the presence of VIC markers, such as vimentin and integrin

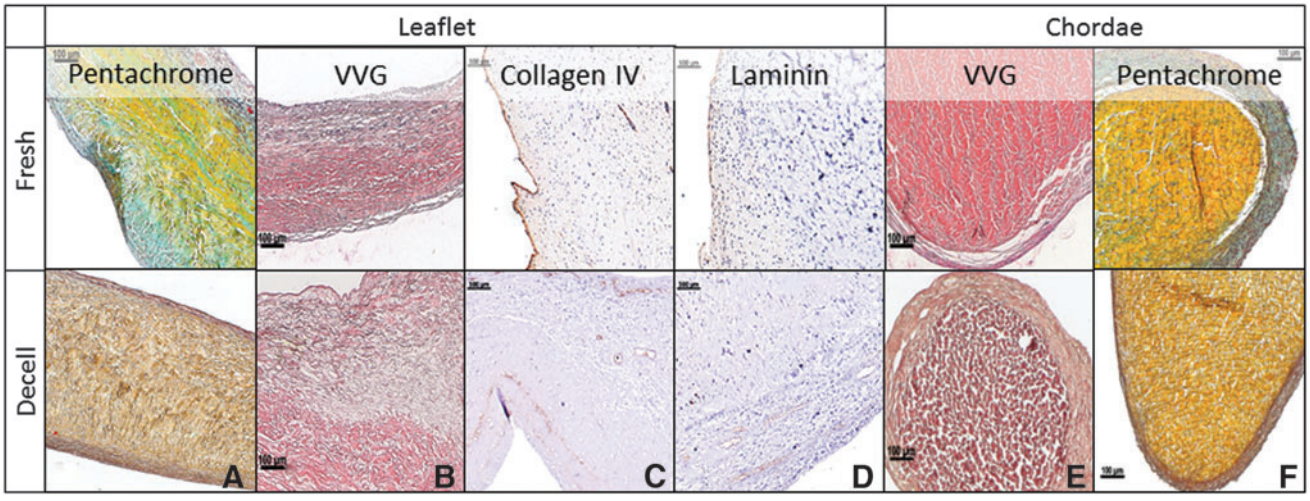

FIG. 2. Histology of mitral valve scaffolds. Representative histology analysis of fresh and decellularized (Decell) mitral valve leaflets and chordae stained with Movats' Pentachrome **(A, F)**, VVG in **(B** and **E)**, and immunohistochemistry for type IV collagen and laminin **(C, D)**. Bars are 100 µm. VVG, Voerhoff van Gieson. Color images available online at www.liebertpub.com/tea

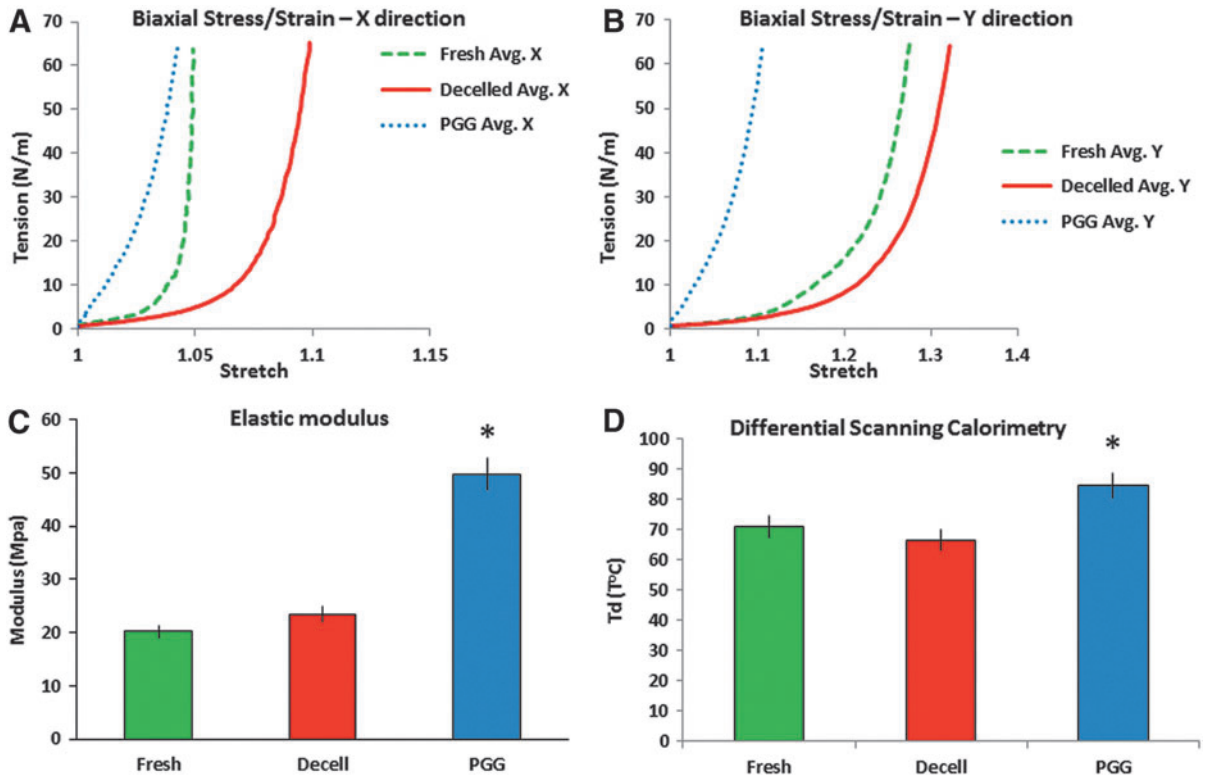

FIG. 3. Matrix stabilization in acellular mitral valves. **(A, B)** Biaxial stress-strain analysis of samples of fresh, acellular (Decelled) and PGG-treated (PGG) acellular valve leaflets tested in radial (X) and circumferential (Y) directions. Avg., average values for $n=5$. **(C)** Elastic moduli of fresh, Decelled and PGG leaflets. **(D)** Differential scanning calorimetry evaluation of fresh, Decelled and PGG-treated acellular valve leaflets. T_d, thermal denaturation temperature. $^*p<0.05$ compared to fresh. PGG, penta-galloyl glucose. Color images available online at www.liebertpub.com/tea

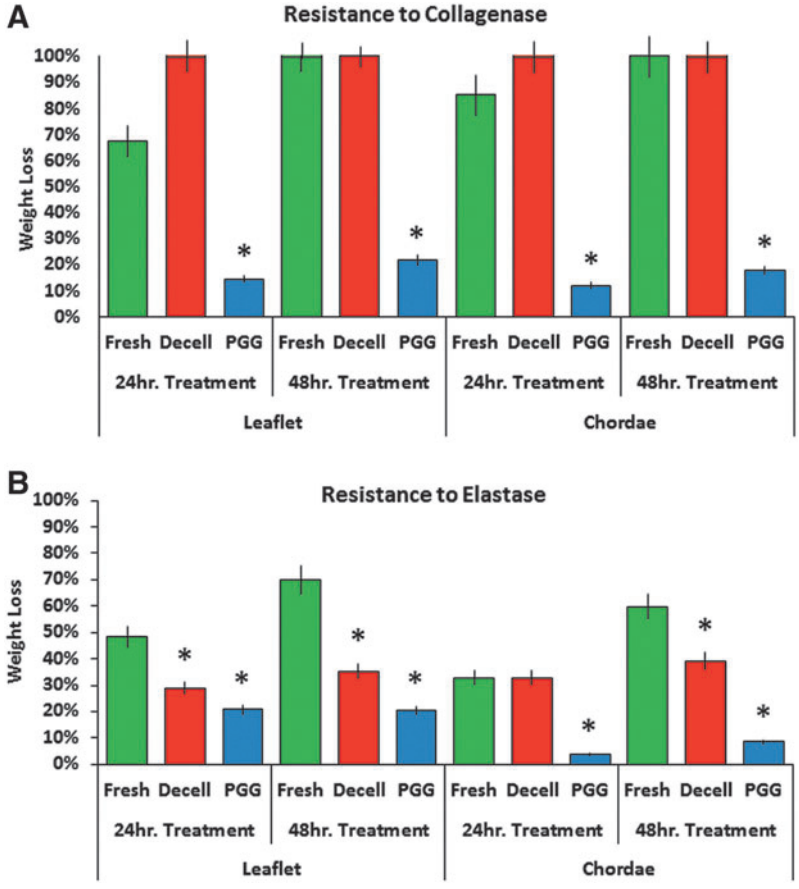

FIG. 4. Resistance to proteases. **(A)** Resistance to collagenase and **(B)** Resistance to elastase degradation of fresh, acellular (Decell) and PGG-treated (PGG) acellular mitral valve leaflets. Values are expressed as % dry weight loss after exposure to enzyme for 24 or 48 h (hr). $^*p<0.05$ compared to fresh. Color images available online at www.liebertpub.com/tea

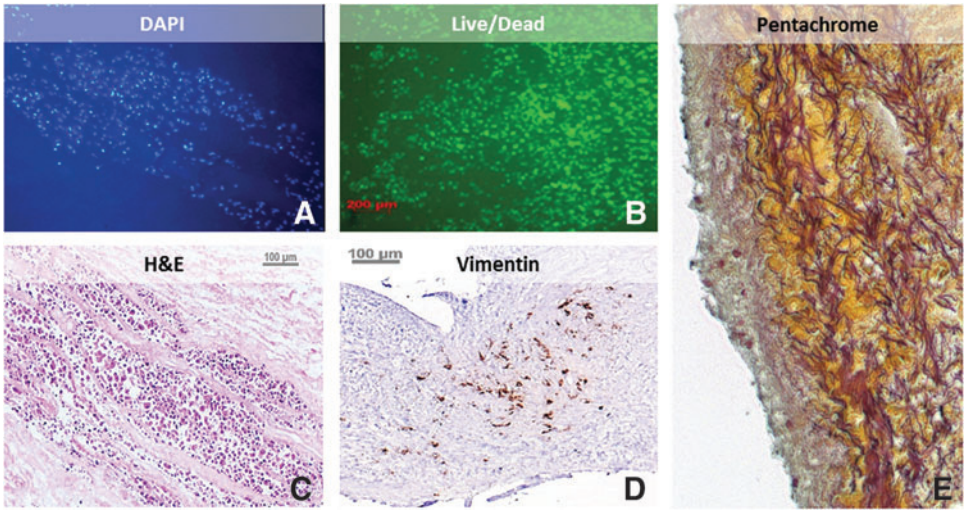

FIG. 5. Cytocompatibility of acellular mitral scaffolds. Representative images of PGG-treated scaffolds seeded with cells and analyzed 3 days after seeding. **(A)** DAPI nuclear staining, **(B)** Live/Dead staining, **(C)** H&E stain, **(D)** vimentin immunohistochemistry and **(E)** Movat's Pentachrome. Bars are 100 μm. Color images available online at www.liebertpub.com/tea

β1, and α-SMA, a marker of smooth muscle cells, cells commonly found in the annular region of the valve (Fig. 6D).

PGG-treated scaffolds and fibroblast activation

To test the effect of scaffolds on fibroblast activation, PGG-treated and untreated scaffolds were seeded with human cardiac fibroblasts and incubated in cell culture medium for 1 week. Fibroblasts seeded on untreated scaffolds became positive for α-SMA and secreted significant amounts of TGF-β (5.5 ± 1.7 pg/μg protein) and high levels of active MMPs (Fig. 7A, B) suggesting their activation into myofibroblasts. By comparison, fibroblasts seeded on PGG-treated scaffolds secreted almost 10 times less TGF-β (0.6 ± 0.1 pg/μg protein) and 2 times less MMPs and were negative for α-SMA (Fig. 7C), suggesting that PGG-mediated stabilization of acellular scaffolds could reduce fibroblast activation. These results were correlated with the reduced level of soluble peptides released by the stabilized scaffold (Fig. 7D), which can act as matrikines and induce fibroblast transformation.

To gain insight into the biocompatibility of acellular MV scaffolds, we implanted samples subdermally in juvenile rats and explanted them after 4 weeks (Fig. 8). All implants showed excellent preservation of the ECM components and mild to moderate host cell infiltration penetrating the outermost 100–200 μm layer. Quantitatively, the extent of cell infiltration was similar in all implants (2575 ± 760 cells per section, not statistically different by ANOVA). Most of the cells appeared fibroblastic in morphology and inflammation was very limited; no foreign body giant cells were observed and no calcification could be detected (not shown). Few CD8-positive cells were found within the population of infiltrating cells (about 10%); notably, the number of CD8-positive cells was significantly reduced in PGG-treated scaffolds compared to nontreated scaffolds (Fig. 8).

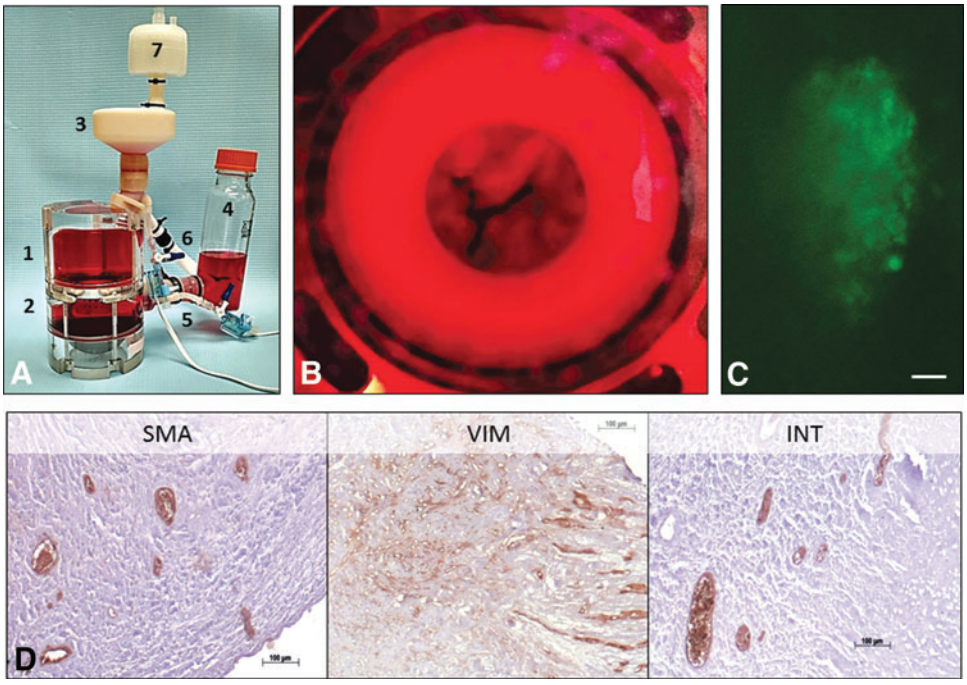

FIG. 6. Bioreactor study. **(A)** Assembled mitral valve bioreactor composed of 1, ventricular chamber, 2, atrial chamber, 3, ventricular reservoir, 4, atrial reservoir, 5, pressure transducer, 6, flow meter, 7, sterile air filter. **(B)** Ventricular aspect of a representative cell-seeded, PGG-treated mitral valve scaffold during testing in culture media (*red*). **(C)** Representative image of Live/Dead (live, *green*, dead, *red*) stained cells after 3 weeks in the mitral valve bioreactor. **(D)** Representative immunohistochemistry images of PGG-treated mitral valve scaffolds seeded with cells and analyzed 3 weeks after bioreactor testing. SMA, α-smooth muscle cell actin, VIM, vimentin, INT, integrin β1. Bars are 100 μm. Color images available online at www.liebertpub.com/tea

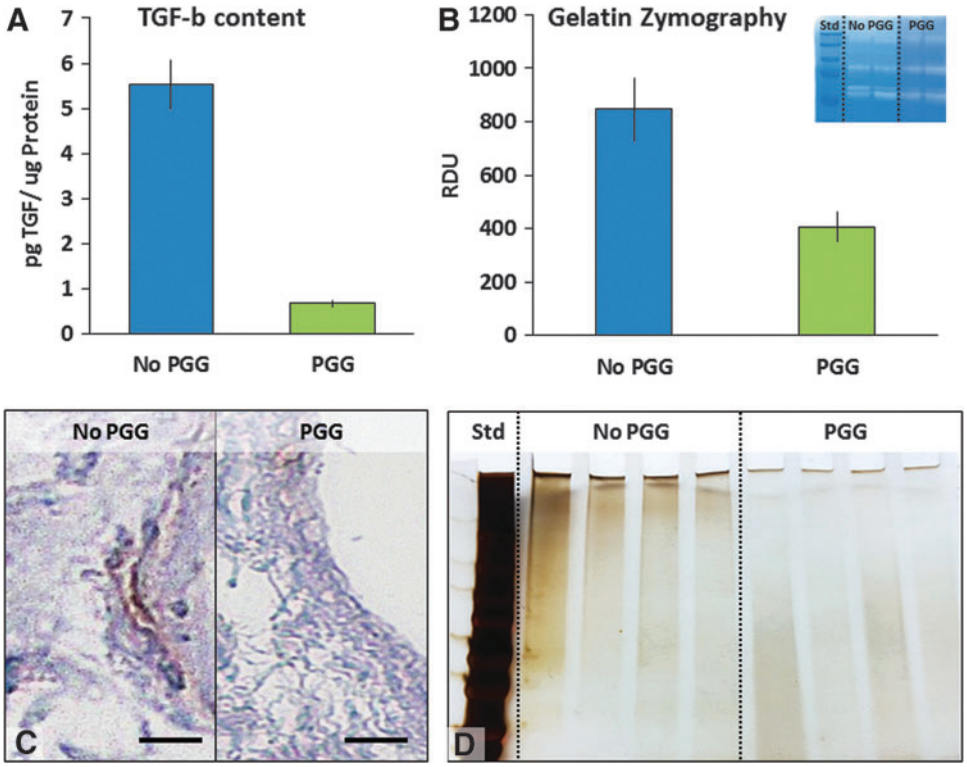

FIG. 7. Effects of PGG stabilization on fibroblast activation. Fibroblasts were seeded onto PGG-treated mitral valve scaffolds (PGG) and their activation compared to cells seeded onto non-PGG-treated scaffolds. **(A)** TGF secretion assessed by ELISA. **(B)** MMP secretion evaluated by zymography (insert shows actual gel). **(C)** Representative immunohistochemistry images of PGG-treated mitral valve scaffolds seeded with cells and stained for SMA. Bars are 100 μm. **(D)** Soluble peptide release assessed by gradient SDS-PAGE followed by silver staining. Std, molecular weight standards. MMP, matrix metalloproteinase. Color images available online at www.liebertpub.com/tea

Discussion

The MV composition and structure, and its pathology, needs to be taken into consideration to develop a robust and functional tissue-engineered MV, resistant to degenerative factors.[3,40] The MV accomplishes a complex and stressful mechanical effort during the cardiac cycle[10,41] that demands the integrity of all the components of the MV apparatus: the anterior leaflet, positioned in a fibrous continuity (fibrous annulus) with the noncoronary leaflets of the aortic valve, and a posterior leaflet, attached through the muscular part of the annulus to the left ventricle; the flexible chordae tendinae, which reinforce the leading edges of both leaflets, and continue with papillary muscles; the papillary muscles that function as shock absorbers and compensate for the geometric changes of the left ventricular wall. This mechanism maintains constant the papillary-annulus distance during the cardiac cycle, while the distance between the papillary

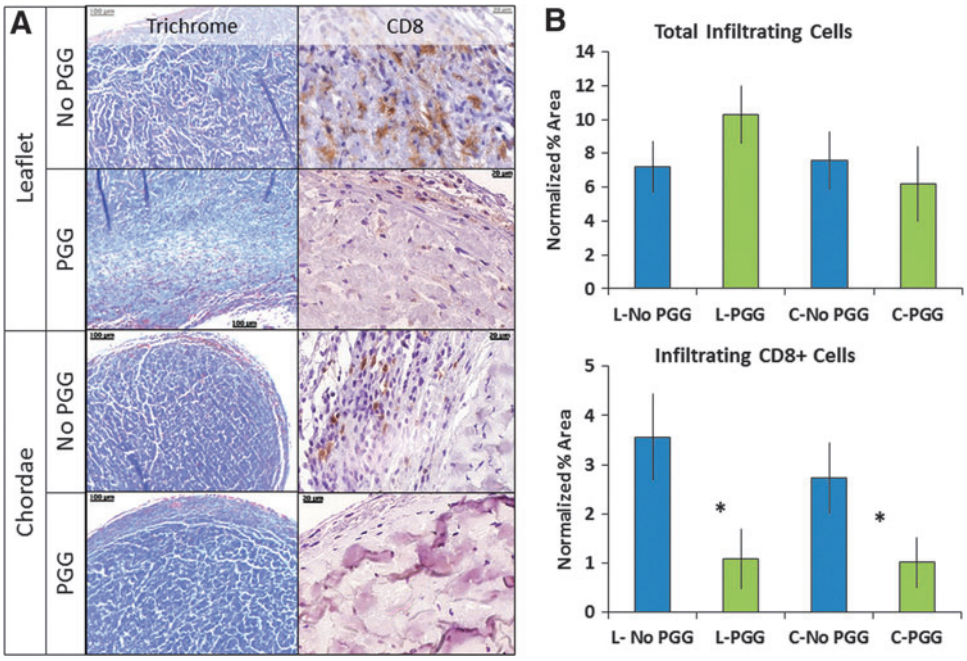

FIG. 8. Effects of PGG on host infiltration into acellular mitral valve scaffolds at 4 weeks postimplantation. **(A)** Representative histology images of leaflet (L) and chordae (C) scaffolds stained with Trichrome (collagen, *blue*; cells, *red*) and anti-CD8 antibody (positive, brown). **(B)** Quantitative analysis of total infiltrating cells (*top*) and CD8+ infiltrating cells (*bottom*), both normalized to scaffold cross-sectional area. Scale bars are 100 μm in Trichrome images and 20 μm in CD8 images. $*p < 0.05$ by ANOVA. ANOVA, analysis of variance. Color images available online at www.liebertpub.com/tea

muscles and the apex varies significantly, due to the presence of chordae, the principal force transmission during left ventricular ejection.[1] The annulus-papillary muscle continuity is essential for the valve mechanics, while the excessive area of the leaflets supports the MV orifice closing; the systolic constriction of the posterior ventricular wall around the annulus also contributes to closing, by narrowing the annulus opening, thus reducing the stress of the leaflets under the LV pressure and flow.[42] This complex mechanical performance of the MV structures requires the integrity and durability of strong collagen[2] and resilient elastin fibers.[18]

It is our working hypothesis that a tissue-engineered MV scaffold, based on stabilized matrix proteins, will demonstrate biochemical and mechanical properties similar to those of the MV leaflets and chordae. Therefore, we developed a durable scaffold by removing all the cellular components of a porcine MV and stabilizing the collagen and elastin fibers with PGG, a polyphenol that binds to the hydrophobic sequences of the polypeptide chains of collagen and elastin. Scaffolds for tissue engineering were successfully developed before, by removal of cells from porcine heart valves.[43,44] Similar to previous work on the aortic and pulmonary valves performed in our lab, we managed to maintain the three-layer structure of the MV leaflets (Figs. 1 and 2), and also of the specific composition of the chordae. The structure of collagen and elastin fibers were preserved in the PGG-treated tissue, together with basement membrane proteins, known for their role in cell repopulation of the scaffold (Fig. 2).

PGG, used before for the stabilization of aortic valve scaffolds, was used here for the first time for the stabilization of the complex and heterogeneous structure of the MV. PGG-treated acellular MV scaffolds showed mechanical properties and cross-linking degrees similar to the fresh MV tissue (Fig. 3). This might be significant for MV durability, as the *in vivo* fragmentation of collagen organization in fibrosa and elastic fibers in the atrialis leads to MV prolapse and insufficiency.[45] The weak and enlarged ''floppy'' leaflets are associated with chordal elongation, thinning, and/or rupture. Indeed, PGG prevents the fragmentation of collagen and elastin fibers and, consequently, the alterations of the mechanical properties (Fig. 3). The increased resistance of PGG-treated scaffolds to the activity of proteases confirms the integrity of these macromolecules (Fig. 4). These results might be truly significant, as it was demonstrated before that fragmented elastin is prone to induce calcification in different cardiovascular tissues, such as the aortic wall and possibly valves.[46] Indeed, varying degrees of calcification are detected in the dilated annulus of the degenerative MVs. In this study, none of the acellular scaffolds accumulated any significant amounts of calcium upon subdermal implantation.

Besides optimal physical properties and three-dimensional (3D) structure, the collagen and elastin-based scaffolds proved to be cytocompatible. As our approach follows the TE paradigm of scaffolds seeded with stem cells and conditioned in a bioreactor, the first step was to test the viability of human ASCs, cultured under static conditions. We noticed that, after 3 months of incubation, not only cells were viable, but they also synthesized a layer of GAGs, which we interpreted as a constructive remodeling of the leaflets (Fig. 5). As cell-matrix interactions continuously determine the ECM remodeling during normal processes, the well-preserved biochemical composition of the scaffold, and its architecture, appeared to have induced a positive remodeling, an encouraging result for MV tissue engineering.

In agreement with studies that showed the expression of integrin β1 in stem cells submitted to mechanical forces,[47,48] we showed that the combined effect of scaffold's 3D structure and mechanical stimuli provided by the bioreactor induced changes in ASC properties, similar to VICs (Fig. 6). These results suggest that bioreactor conditions are appropriate for the development of a tissue-engineered MV.

In addition, we studied the activation of human fibroblasts seeded on PGG-treated and untreated MV scaffolds by evaluating the synthesis of MMPs and TGF-β1, and by staining for α-SMA. As collagen and elastin peptides are known to be involved in myofibroblast generation, we correlated the MMP, TGF-β1, and α-SMA with the amount of peptides released by the scaffold ECM (Fig. 7). Our results showed that PGG-treated scaffolds released only a reduced amount of peptides compared to nontreated scaffolds, suggesting that PGG-treated scaffolds mitigate the activation of fibroblasts to myofibroblasts. Furthermore, as shown in our *in vivo* studies, PGG treatment of acellular scaffolds reduced the extent of T-lymphocyte infiltration suggesting that PGG might exert anti-inflammatory properties.[35]

Therefore, by maintaining the ECM structural integrity, PGG might prevent the activation of valvular cells, and consequently the weakening of tissue-engineered MV, dysfunction, and disease. The study of tissue-engineered MV under bioreactor conditions could serve as a reliable *in vitro* model for studying MV biology and pathology. Definitely, bioreactor studies could provide an insightful understanding of how the valve microstructural alterations represent an early effort to compensate for altered physiologic loading to reduce stress and maintain leaflet coaptation.

Conclusions

Stabilized acellular MV scaffolds serve as suitable foundations for tissue regeneration. PGG, by virtue of its collagen and elastin-stabilizing abilities preserves the ECM composition and structure, required by the valve's complex mechanical efforts. This could prevent weakening of the leaflets and chordae under mechanical stress and also protect the scaffolds from degeneration, inflammation, foreign body reactions, and calcification. Acellular MV scaffolds are highly biocompatible *in vitro* and *in vivo*; furthermore, PGG treatment of these mitigates fibroblast activation, inflammation, and calcification. In future *in vivo* studies, we anticipate to show that PGG-treated scaffolds will not only provide the proper mechanical support for cells, but also the appropriate biochemical environment to prevent their activation and calcification.

Acknowledgments

The authors wish to thank Snow Creek Abattoir, SC for providing the porcine hearts. This project was funded in part by NIGMS of the National Institutes of Health under award number 5P20GM103444-07 (to A.S.), by the Harriet and Jerry Dempsey Bioengineering Professorship Award (to D.S.) and by a grant from the Romanian National Authority for Scientific Research, CNCS-UEFISCDI, project number PNII-ID-PCCE-2011-2-0036 (to A.S., D.S.).

Disclosure Statement

No competing financial interests exist.

References

1. Di Mauro, M., Gallina, S., D'Amico, M.A., Izzicupo, P., Lanuti, P., Bascelli, A., Di Fonso, A., Bartoloni, G., Calafiore, A.M., and Di Baldassarre, A. Functional mitral regurgitation: from normal to pathological anatomy of mitral valve. Int J Cardiol **163,** 242, 2013.
2. Kunzelman, K.S., Quick, D.W., and Cochran, R.P. Altered collagen concentration in mitral valve leaflets: biochemical and finite element analysis. Ann Thorac Surg **66,** S198, 1998.
3. Schoen, F.J. Evolving concepts of cardiac valve dynamics: the continuum of development, functional structure, pathobiology, and tissue engineering. Circulation **118,** 1864, 2008.
4. Chester, A.H., and Taylor, P.M. Molecular and functional characteristics of heart-valve interstitial cells. Philos Trans R Soc Lond B Biol Sci **362,** 1437, 2007.
5. Filip, D.A., Radu, A., and Simionescu, M. Interstitial cells of the heart valves possess characteristics similar to smooth muscle cells. Circ Res **59,** 310, 1986.
6. Cushing, M.C., Liao, J.T., and Anseth, K.S. Activation of valvular interstitial cells is mediated by transforming growth factor-beta1 interactions with matrix molecules. Matrix Biol **24,** 428, 2005.
7. Merryman, W.D., Huang, H.Y., Schoen, F.J., and Sacks, M.S. The effects of cellular contraction on aortic valve leaflet flexural stiffness. J Biomech **39,** 88, 2006.
8. Merryman, W.D., Youn, I., Lukoff, H.D., Krueger, P.M., Guilak, F., Hopkins, R.A., and Sacks M.S. Correlation between heart valve interstitial cell stiffness and transvalvular pressure: implications for collagen biosynthesis. Am J Physiol Heart Circ Physiol **290,** H224, 2006.
9. Balachandran, K., Sucosky, P., Jo, H., and Yoganathan, A.P. Elevated cyclic stretch alters matrix remodeling in aortic valve cusps: implications for degenerative aortic valve disease. Am J Physiol Heart Circ Physiol **296,** H756, 2009.
10. Richards, J.M., Farrar, E.J., Kornreich, B.G., Moïse, N.S., and Butcher J.T. The mechanobiology of mitral valve function, degeneration, and repair. J Vet Cardiol **14,** 47, 2012.
11. Lee, C.H., Carruthers, C.A., Ayoub, S., Gorman, R.C., Gorman, J.H., 3rd, and Sacks, M.S. Quantification and simulation of layer-specific mitral valve interstitial cells deformation under physiological loading. J Theor Biol **373,** 26, 2015.
12. Freed, L.A., Levy, D., Levine, R.A., Larson, M.G., Evans, J.C., Fuller, D.L., Lehman, B., and Benjamin, E.J. Prevalence and clinical outcome of mitral-valve prolapse. N Engl J Med **341,** 1, 1999.
13. Levine, R.A., Hagege, A.A., Judge, D.P., Padala, M., Dal-Bianco, J.P., Aikawa, E., Beaudoin, J., Bischoff, J., Bouatia-Naji, N., Bruneval, P., Butcher, J.T., Carpentier, A., Chaput, M., Chester, A.H., Clusel, C., Delling, F.N., Dietz, H.C., Dina, C., Durst, R., Fernandez-Friera, L., Handschumacher, M.D., Jensen, M.O., Jeunemaitre, X.P., Marec, H.L., Tourneau, T.L., Markwald, R.R., Merot, J., Messas, E., Milan, D.P., Neri, T., Norris, R.A., Peal, D., Perrocheau, M., Probst, V., Puceat, M., Rosenthal, N., Solis, J., Schott, J.J., Schwammenthal, E., Slaugenhaupt, S.A., Song, J.K., and Yacoub, M.H. Mitral valve disease-morphology and mechanisms. Nat Rev Cardiol **12,** 689, 2015.
14. Adams, D.H., Rosenhek, R., and Falk, V. Degenerative mitral valve regurgitation: best practice revolution. Eur Heart J **31,** 1958, 2010.
15. Prunotto, M., Caimmi, P.P., and Bongiovanni, M. Cellular pathology of mitral valve prolapse. Cardiovasc Pathol **19,** e113, 2010.
16. Icardo, J.M., Colvee, E., and Revuelta, J.M. Structural analysis of chordae tendineae in degenerative disease of the mitral valve. Int J Cardiol **167,** 1603, 2013.
17. Carpentier, A.F., Pellerin, M., Fuzellier, J.F., and Relland, J.Y. Extensive calcification of the mitral valve anulus: pathology and surgical management. J Thorac Cardiovasc Surg **111,** 718, 1996; discussion 729–730.
18. Tamura, K., Fukuda, Y., Ishizaki, M., Masuda, Y., Yamanaka, N., and Ferrans, V.J. Abnormalities in elastic fibers and other connective-tissue components of floppy mitral valve. Am Heart J **129,** 1149, 1995.
19. Grande-Allen, K.J., Griffin, B.P., Ratliff, N.B., Cosgrove, D.M., and Vesely, I. Glycosaminoglycan profiles of myxomatous mitral leaflets and chordae parallel the severity of mechanical alterations. J Am Coll Cardiol **42,** 271, 2003.
20. Walker, G.A., Masters, K.S., Shah, D.N., Anseth, K.S., and Leinwand, L.A. Valvular myofibroblast activation by transforming growth factor-beta: implications for pathological extracellular matrix remodeling in heart valve disease. Circ Res **95,** 253, 2004.
21. Caulfield, J.B., Page, D.L., Kastor, J.A., and Sanders, C.A. Connective tissue abnormalities in spontaneous rupture of chordae tendineae. Arch Pathol **91,** 537, 1971.
22. Messier, R.H., Jr., Bass, B.L., Aly, H.M., Jones, J.L., Domkowski, P.W., Wallace, R.B., and Hopkins, R.A. Dual structural and functional phenotypes of the porcine aortic valve interstitial population: characteristics of the leaflet myofibroblast. J Surg Res **57,** 1, 1994.
23. Simionescu, A., Simionescu, D.T., and Deac, R.F. Matrix metalloproteinases in the pathology of natural and bioprosthetic cardiac valves. Cardiovasc Pathol **5,** 323, 1996.
24. Rabkin, E., Aikawa, M., Stone, J.R., Fukumoto, Y., Libby, P., and Schoen, F.J. Activated interstitial myofibroblasts express catabolic enzymes and mediate matrix remodeling in myxomatous heart valves. Circulation **104,** 2525, 2001.
25. Hagler, M.A., Hadley, T.M., Zhang, H., Mehra, K., Roos, C.M., Schaff, H.V., Suri, R.M., and Miller, J.D. Tgf-beta signalling and reactive oxygen species drive fibrosis and matrix remodelling in myxomatous mitral valves. Cardiovasc Res **99,** 175, 2013.
26. Mott, J.D., and Werb, Z. Regulation of matrix biology by matrix metalloproteinases. Curr Opin Cell Biol **16,** 558, 2004.
27. Gu, X., and Masters, K.S. Regulation of valvular interstitial cell calcification by adhesive peptide sequences. J Biomed Mater Res A **93,** 1620, 2010.
28. Grande-Allen, K.J., and Liao, J. The heterogeneous biomechanics and mechanobiology of the mitral valve: implications for tissue engineering. Curr Cardiol Rep **13,** 113, 2011.
29. Deac, R.F., Simionescu, D., and Deac, D. New evolution in mitral physiology and surgery: mitral stentless pericardial valve. Ann Thorac Surg **60,** S433, 1995.
30. Isenburg, J.C., Simionescu, D.T., and Vyavahare, N.R. Elastin stabilization in cardiovascular implants: improved resistance to enzymatic degradation by treatment with tannic acid. Biomaterials **25,** 3293, 2004.

31. Isenburg, J.C., Karamchandani, N.V., Simionescu, D.T., and Vyavahare, N.R. Structural requirements for stabilization of vascular elastin by polyphenolic tannins. Biomaterials **27,** 3645, 2006.
32. Isenburg, J.C., Simionescu, D.T., Starcher, B.C., and Vyavahare, N.R. Elastin stabilization for treatment of abdominal aortic aneurysms. Circulation **115,** 1729, 2007.
33. Tedder, M.E., Liao, J., Weed, B., Stabler, C., Zhang, H., Simionescu, A., and Simionescu, D.T. Stabilized collagen scaffolds for heart valve tissue engineering. Tissue Eng Part A **15,** 1257, 2009.
34. Tedder, M.E., Simionescu, A., Chen, J., Liao, J., and Simionescu, D.T. Assembly and testing of stem cell-seeded layered collagen constructs for heart valve tissue engineering. Tissue Eng Part A **17,** 25, 2011.
35. Zhang, J., Li L., Kim, S.H., Hagerman, A.E., and Lu, J. Anti-cancer, anti-diabetic and other pharmacologic and biological activities of penta-galloyl-glucose. Pharm Res **26,** 2066, 2009.
36. Chuang, T.H., Stabler, C., Simionescu, A., and Simionescu, D.T. Polyphenol-stabilized tubular elastin scaffolds for tissue engineered vascular grafts. Tissue Eng Part A **15,** 2837, 2009.
37. Liao, J., Joyce, E.M., and Sacks, M.S. Effects of decellularization on the mechanical and structural properties of the porcine aortic valve leaflet. Biomaterials **29,** 1065, 2008.
38. Chow, J.P., Simionescu, D.T., Warner, H., Wang, B., Patnaik, S.S., Liao, J., and Simionescu, A. Mitigation of diabetes-related complications in implanted collagen and elastin scaffolds using matrix-binding polyphenol. Biomaterials **34,** 685, 2013.
39. Sierad, L.N., Simionescu, A., Albers, C., Chen, J., Maivelett, J., Tedder, M.E., Liao, J., and Simionescu, D.T. Design and testing of a pulsatile conditioning system for dynamic endothelialization of polyphenol-stabilized tissue engineered heart valves. Cardiovasc Eng Technol **1,** 138, 2010.
40. Vesely, I. Heart valve tissue engineering. Circ Res **97,** 743, 2005.
41. Rausch, M.K., Famaey, N., Shultz, T.O., Bothe, W., Miller, D.C., and Kuhl, E. Mechanics of the mitral valve: a critical review, an in vivo parameter identification, and the effect of prestrain. Biomech Model Mechanobiol **12,** 1053, 2013.
42. Hasenkam, J.M., Nygaard, H., Paulsen, P.K., Kim, W.Y., and Hansen, O.K. What force can the myocardium generate on a prosthetic mitral valve ring? An animal experimental study. J Heart Valve Dis **3,** 324, 1994.
43. Sierad, L.N., Shaw, E.L., Bina, A., Brazile, B., Rierson, N., Patnaik, S.S., Kennamer, A., Odum, R., Cotoi, O., Terezia, P., Branzaniuc, K., Smallwood, H., Deac, R., Egyed, I., Pavai, Z., Szanto, A., Harceaga, L., Suciu, H., Raicea, V., Olah, P., Simionescu, A., Liao, J., Movileanu, I., Harpa, M., and Simionescu, D.T. Functional heart valve scaffolds obtained by complete decellularization of porcine aortic roots in a novel differential pressure gradient perfusion system. Tissue Eng Part C Methods **21,** 1284, 2015.
44. Iablonskii, P., Cebotari, S., Tudorache, I., Granados, M., Morticelli, L., Goecke, T., Klein, N., Korossis, S., Hilfiker, A., and Haverich, A. Tissue-engineered mitral valve: morphology and biomechanics dagger. Interact Cardiovasc Thorac Surg **20,** 712, 2015; discussion 719.
45. Salhiyyah, K., Yacoub, M.H., and Chester, A.H. Cellular mechanisms in mitral valve disease. J Cardiovasc Transl Res **4,** 702, 2011.
46. Simionescu, A., Simionescu, D.T., and Vyavahare, N.R. Osteogenic responses in fibroblasts activated by elastin degradation products and transforming growth factor-beta1: role of myofibroblasts in vascular calcification. Am J Pathol **171,** 116, 2007.
47. Latif, N., Sarathchandra, P., Taylor, P.M., Antoniw, J., and Yacoub, M.H. Molecules mediating cell-ecm and cell-cell communication in human heart valves. Cell Biochem Biophys **43,** 275, 2005.
48. Stephens, E.H., Durst, C.A., West, J.L., and Grande-Allen, K.J. Mitral valvular interstitial cell responses to substrate stiffness depend on age and anatomic region. Acta Biomater **7,** 75, 2011.

Address correspondence to:
Agneta Simionescu, PhD
Department of Bioengineering
Clemson University
301 Rhodes Hall
Clemson, SC 27631

E-mail: agneta@clemson.edu

Received: January 22, 2016
Accepted: August 29, 2016
Online Publication Date: October 3, 2016